Interconnect Mode Conversion in High-Speed VLSI Circuits

Y. Quéré*, T. LeGouguec, P.M. Martin, F. Huret
Laboratoire d'Electronique et Systèmes de Télécommunications – Université de Bretagne Occidentale U.M.R CNRS 6165, 6 Avenue le Gorgeu, CS93879, 29238 Brest Cedex 3, France.
**Yves.quere@univ-brest.fr*

Abstract

A modification of the Electromagnetic Field configuration (mode conversion) at interconnect discontinuities in deep submicron digital ULSI circuits was investigated by using a Full Wave Electromagnetic Analysis. The mode conversion analysis is indispensable to identify the signal return path, the return current distribution and therefore for an accurate inductance modeling which remains a challenging problem. On the other hand, switching activity of high speed CMOS circuit may produce large current derivatives. These transient currents can generate large potential surges and coupled noise due to the parasitic resistances and inductances of the wires. In this aim, we determined a simple design rule to reduce the mode conversion phenomenon and, therefore, decrease noise in high-speed ULSI circuits.

1. Introduction

Microelectronics evolution is characterized by an important rise in integration and circuit speed running. Today, the race towards integration is slowed down by the problem of interconnects which blocks improvement in circuit performances. Indeed, routing the signal between the hundreds of millions of transistors on a chip without generating too much parasitic effects is more and more difficult. Accurate prediction of propagation delay, crosstalk and pulse distortion in high-speed interconnects is strongly dependent on the per-unit parameters model accuracy. For example, compared to an RLC model, an RC one may generate an error of up to 30% of the total repeater system one [1]. In the same way, because of the continuing advancements in process technology, one may expect an enhancement of substrate effect [2]. A decrease in the feature size to deep submicrom dimensions results in more significant coupling effects: indeed, the spacing between conductor lines is lowered; moreover, the conductors thickness is increased to reduce their parasitic resistance. An analysis of the coupling noise can be performed in the frequency and time domains; the electrical phenomena to be investigated are governed by the electromagnetic theory. Thus, designers will obviously need to enter the world of electromagnetic field.

Therefore, the study of the coupling characteristics of the substrate as well as the crosstalk and noise reduction techniques, are becoming more and more important [3].

Many investigations have demonstrated and explained the great interest of SOI devices for substrate crosstalk reduction [4-5]. Nevertheless, the optimization of the substrate behavior from a crosstalk point of view is not the only way to do it. Circuit design rules can also reduce the risk of substrate crosstalk [6]. In this context, it is well known that it is better to design analog differential devices. For digital circuits, due to logical and physical considerations, designers put ground lines near signal ones and within the same metal layer to get a differential configuration rather than a common one. This case is illustrated in Fig.1b, where arrows depict the coupling between the two wires. From an electromagnetic point of view, it means that one should excite the differential (odd mode) mode rather than the common one (even mode): in the latter, the substrate acts as a ground plane, and thus the return longitudinal currents in the substrate as well as the shunt currents can both give rise to a significant substrate crosstalk.

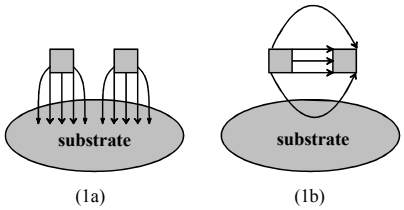

Fig.1 Electric field configuration of the two possible modes
Fig.1a: common (even) mode
Fig.1b: differential (odd) mode

However, according to several studies asymmetric discontinuities in microwave circuits lead to a mode conversion [7, 8, 9]. This means that, after a discontinuity of interconnects like a transition between two metal layers, excitation of the differential mode, for example, may result in the transmission of all the power via the common mode. Thus, mode conversion at interconnect discontinuities in Digital ULSI circuits needs further investigations to determine simple design rules for substrate crosstalk and noise reduction. From another point of view, the mode conversion analysis is indispensable to identify the signal return path, the return current distribution and therefore for an accurate

0-7695-2093-6/04 $20.00 © 2004 IEEE

inductance modeling which remains a challenging issue in new generation of VLSI and ULSI circuits.

All these considerations led us to investigate simple, though generic, structures with two or three copper coupled lines, SILK dielectric, and SiN passivation. Considering a complete circuit does not allow one to grasp the physical mechanisms that rule the phenomena of concern, and therefore to find ways to reduce the mode conversion. The mode conversion shows a transformation of Electric (and Magnetic) Field orientation of the propagation in the guided structure. Figures 2 and 3 respectively depict the different Electric Field configurations of the two, or three, possible modes for two, or three, coupled lines above an equivalent ground plane, which can represent a very dense lower metal layer or the doped silicon substrate.

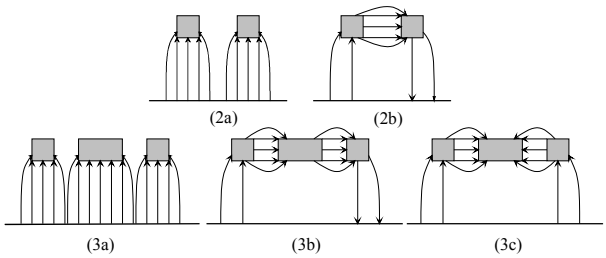

Fig.2 E-field configuration of the two possible modes
Fig2a: differential mode
Fig2b: common mode
Fig.3 E-field configuration of the three possible modes
Fig3a: « microstrip » mode
Fig3b: antisymmetric mode
Fig3c: symmetric mode

Section 2 of this paper introduces the mode conversion theory in the case of two coupled interconnects. The full wave electromagnetic analysis required for the scattering and RLCG parameters is developed in Section 3. Section 4 analyzes the mode conversion for two kinds of discontinuities representing two types of transition between two different layers. One of the two wires, the ground or signal line, is longer than the another one. The transient analysis demonstrates the influence of the mode conversion on signal integrity and validates the design rule proposed to reduce this phenomenon. Section 5 is devoted to three-coupled-wire transitions between two metal layers. Conclusions are drawn in Section 6.

2. Mode conversion theory

By using a 3-D full wave electromagnetic analysis, this multiple-port scattering problem is described by *s*-parameters, but a modification of existing generalized *s*-parameters is needed to evidence the mode conversion. We illustrate this theory on a two-coupled-interconnect structure above a ground plane. In this case, two TEM modes, *i.e.* differential and common ones, can propagate. These physical two-port structure can be drawn as a traditional virtual four-port structure (Fig.4) where the two modes are separated. It is worth noting that ports are only conceptual tools, and not physically separated entities.

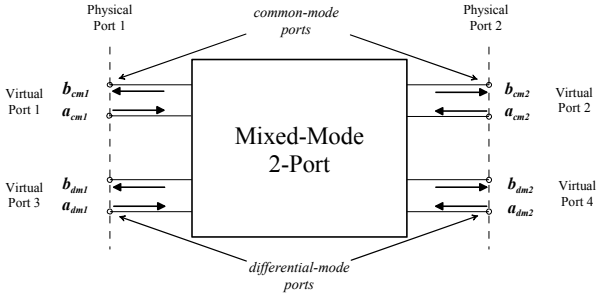

Fig.4: Conceptual diagram of mixed-mode two-port

In the conceptual diagram represented in Fig. 4 the letter *b* indicates the outgoing wave and *a* the incoming wave. The subscripts *cm* and *dm* denote common mode and differential mode, respectively. For example, let us call b_{mc1} the outgoing common wave on the physical port 1 and a_{md2} the incoming wave on the physical port 2. The definition of generalized *s*-parameters is:

$$[b] = [S].[a] \qquad (1)$$

where [*b*] and [*a*] denote an n-dimensional column vector and [*S*] is a n-by-n matrix. Given a two-coupled interconnect two-port structure, the generalized mixed-mode *s*-parameters can be expressed as:

$$\begin{aligned} b_{mc1} &= S_{11}a_{mc1} + S_{12}a_{mc2} + S_{13}a_{md1} + S_{14}a_{md2} \\ b_{mc2} &= S_{21}a_{mc1} + S_{22}a_{mc2} + S_{23}a_{md1} + S_{24}a_{md2} \\ b_{md1} &= S_{31}a_{mc1} + S_{32}a_{mc2} + S_{33}a_{md1} + S_{34}a_{md2} \\ b_{md2} &= S_{41}a_{mc1} + S_{42}a_{mc2} + S_{43}a_{md1} + S_{44}a_{md2} \end{aligned} \qquad (2)$$

and the generalized *s*-matrix referenced to virtual port on this device is :

$$[S] = \begin{bmatrix} S_{11} & S_{12} & S_{13} & S_{14} \\ S_{21} & S_{22} & S_{23} & S_{24} \\ S_{31} & S_{32} & S_{33} & S_{34} \\ S_{41} & S_{42} & S_{43} & S_{44} \end{bmatrix} \qquad (3)$$

Where the subscript 1, 2, 3 and 4 denote port 1, 2, 3 and 4 respectively. [*S*] can be describe by :

$$[S] = \left[\begin{array}{c|c} S_{com-com} & S_{com-diff} \\ \hline S_{diff-com} & S_{diff-diff} \end{array}\right] \qquad (4)$$

In the following we will call [$S_{com\text{-}com}$] the common *s*-parameters, [$S_{diff\text{-}diff}$] the differential *s*-parameters and

[$S_{com\text{-}diff}$] and [$S_{diff\text{-}com}$] the mode-conversion or cross-mode *s*-parameters. In particular, [$S_{com\text{-}diff}$] describes the conversion of differential mode waves into common-mode waves, and [$S_{diff\text{-}com}$] describes the conversion of common waves into differential waves. The mixed-mode matrix is:

$$[S]=\begin{bmatrix} S_{11com-com} & S_{12com-com} & S_{11com-diff} & S_{12com-diff} \\ S_{21com-com} & S_{22com-com} & S_{21com-diff} & S_{22com-diff} \\ S_{11diff-com} & S_{12diff-com} & S_{11diff-diff} & S_{12diff-diff} \\ S_{21diff-com} & S_{22diff-com} & S_{21diff-diff} & S_{22diff-diff} \end{bmatrix} \quad (5)$$

This matrix (5) is referenced by physical ports. Thus, $S_{12diff\text{-}com}$ relates the outgoing wave b_{md1} to the incoming wave a_{mc2}. This parameter corresponds to a transmission coefficient between physical ports 2 and 1; $S_{11diff\text{-}diff}$, which represents a reflection coefficient on port 1, relates the outgoing wave b_{md1} to the incoming wave a_{md1}. This study can be easily applied to a 2-port structure where n modes can propagate.

3. Full Wave Electromagnetic Analysis

The electromagnetic analysis of VLSI circuit interconnect consists in the determination of the scattering parameters and propagation characteristics of the guided modes in the corresponding waveguide. Interconnect cross-sectional surfaces are inhomogeneous, and according to Maxwell's equations all the propagating modes are hybrid. Therefore, a Full-Wave analysis is needed to take into account all the effects. The finite element method is probably the waveguide analysis, which is the most generally applicable and versatile procedure. This method divides the studies structure into sub-domains where the Helmoltz equation is solved. The method used here is a Vector Finite Elements (HFSS™ from *Ansoft*) one in order to determine the scattering parameters, the complex propagation factor, the electromagnetic field distribution and the characteristic impedance of the considered waveguide [10]. Each medium of the structure is characterized by a complex permittivity and permeability, so metallic losses and substrate effects are naturally taken account by the finite element method.

In Sections 4 and 5 the interconnects for the two layers will be 1.5-mm-long for each of the studied structures.

4. Mode conversion at two interconnects discontinuities

This section deals with the two structures shown in Figs. 5 and 7.

The mode conversion between the two modes will be neglected if its parameters, *e.g.* $S_{21diff\text{-}com}$, are small compared to the other scattering parameters such as $S_{21diff\text{-}diff}$. This is illustrated in Fig.6 where there is no mode conversion for the 90° bend discontinuity between two different layers depicted in Fig. 5.

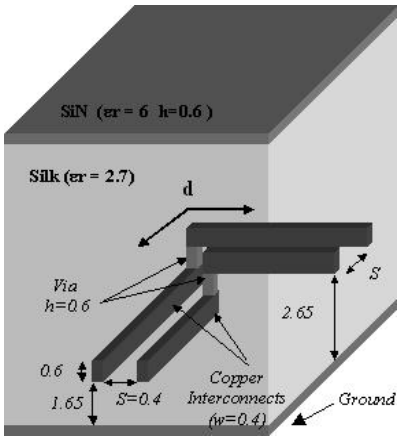

Fig.5 90° bend on two coupled interconnects

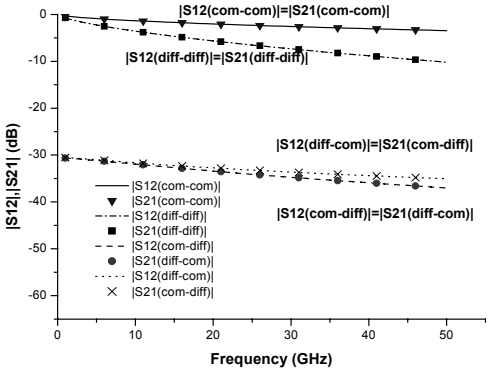

Fig.6 Magnitude of Mixed Mode transmission *s*-parameters for a 90° bend on two coupled interconnects

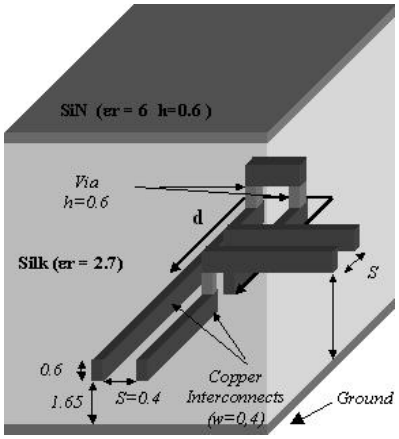

Fig.7 Geometry of a metal layer transition on two coupled interconnects

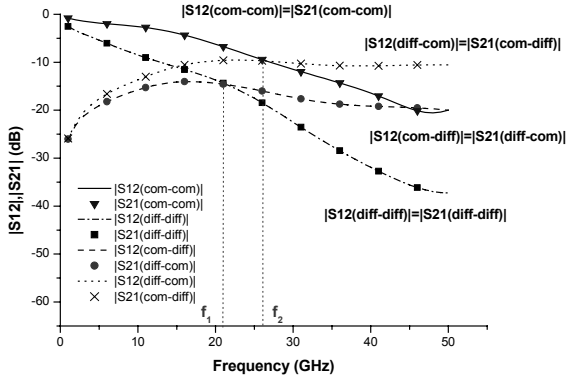

Fig.8 Magnitude of Mixed Mode transmission *s*-parameters for a geometry of a metal layer transition

The reciprocity theorem is respected. Indeed, for example, $S_{12diff\text{-}com}=S_{21com\text{-}diff}$ and $S_{12com\text{-}com}=S_{21com\text{-}com}$. For each discontinuity, we took into account two access lines of 1.5-mm-long on both sides of the discontinuity, which explains the attenuation of the transmission *s*-parameters. In the second example (Fig.7), for the differential mode propagation, the mode conversion phenomenon, due to the discontinuity, becomes more important than the mode transmission at frequencies higher than f_1. As for the common mode propagation, this is also verified when the frequency is higher than f_2 (Fig.8). In this case-study the path difference d is equal to 1.5 mm.

Mode conversion is critical in the frequency range where the path difference between the outer and inner wires is close to one-quarter of the associated wave guide wavelength of the wire:

$$\frac{d}{\lambda_g} = 0.25 \quad (6)$$

The guided wavelength (λ_g) can be expressed with respect to frequency. By considering the useful frequency bandwidth of a signal, the critical path difference, d, may be written as:

$$d < \frac{c.t_r}{1.4\sqrt{\varepsilon_{reff}}} \qquad (7)$$

where c is the light velocity, t_r is the rise time of the propagated signal, e_{reff} represents the relative effective permittivity of the wire equivalent wave guide, easily obtained by a classical 2-D electromagnetic analysis of the device. Whenever equation (7) is verified, the mode conversion can be neglected. We systematically checked it on other examples.

Focus now will be on the mode conversion in time domain. This study illustrates how mode conversion may affect the correct operation of the transistors, and thus of the whole circuit. First, in order to accurately take into account the difference between the two interconnect layers, we extracted RLCG parameters for each of them (Fig.9). These cells were simulated by circuit simulator ADS™ from *Agilent Technology*.

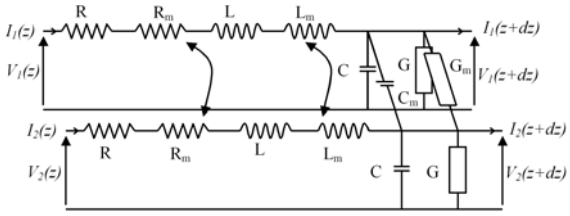

Fig.9 TEM transmission lines model of two coupled interconnects

This transient simulation permitted us to simulate the output common voltage for various lengths of one of the two interconnects when the differential mode was excited. Figure 10 presents the excitation of the two modes.

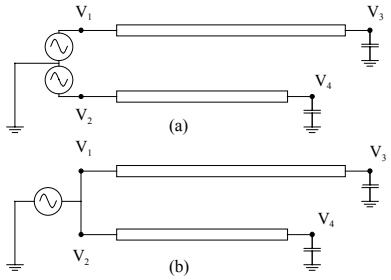

Fig.10 Mixed Mode circuit simulation
Fig.10a: differential voltage
Fig.10b: common voltage

Figure 11 gives the simulation data of a common output signal V_{comp2} for a differential input signal V_{diffp1}. This simulation was carried out on taking into account an electrical model of the buffer to get the differential signal, and then precise the shape of the transistors-delivered signal.

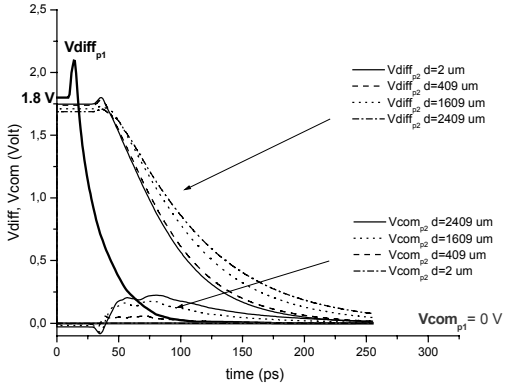

Fig.11 Common output analysis for a differential input

The higher the path difference is, the bigger the common signal magnitude is. It means that the path difference should be rather small to reduce coupled noise and clearly identify the return current path.

5. Mode conversion at three interconnects discontinuities

In this section the mode conversion is studied in the case of three coupled lines. For the considered structure, figure 12, the set of three interconnects can propagate support three dominant quasi-TEM modes. The mode conversion can be described by matrix [*S*] (9) where [$S_{mic\text{-}mic}$] are the "microstrip" *s*-parameters, [$S_{as\text{-}as}$] are the antisymmetric *s*-parameters, [$S_{s\text{-}s}$] are the symmetric s-parameters, [$S_{mic\text{-}s}$], [$S_{s\text{-}mic}$], [$S_{mic\text{-}as}$], [$S_{as\text{-}mic}$], [$S_{s\text{-}as}$] and [$S_{as\text{-}s}$] are the mode-conversion or cross-mode s-parameters.

$$[S]=\begin{bmatrix} S_{mic-mic} & S_{mic-as} & S_{mic-s} \\ S_{as-mic} & S_{as-as} & S_{as\_s} \\ S_{s-mic} & S_{s-as} & S_{s-s} \end{bmatrix} \qquad (9)$$

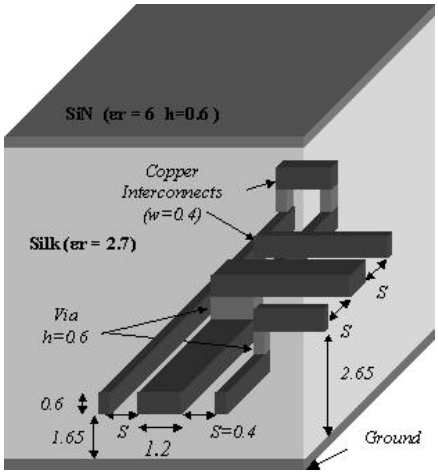

Fig.12 Geometry of a metal layer transition on three coupled interconnects

In this respect, the propagated symmetric mode and the associate cross-mode constitute the interesting points because of the fields configuration (Fig.3). But, the study of the characteristics of others propagation modes allows one to understand mode conversion phenomenon. Since, in the case of a 90°-bend, the level of the cross-mode magnitudes is very small with respect to the mode propagations, there is no conversion mode with three coupled interconnects like in the case of two coupled line. The second example corresponds to an alike structure with a 1.5-mm path difference (Fig.12). Figures 13, 14 and 15 present the frequency evolution of the magnitude of mode transmission *s*-parameters and the associated cross-mode.

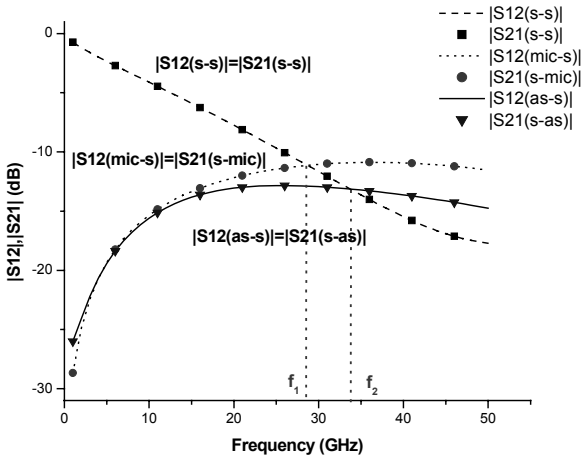

Fig.13 Magnitude of Mixed Mode transmission *s*-parameters of a metal layer transition on three coupled interconnects, symmetric–mode transmission $S_{21(s\text{-}s)}$ and the cross-modes transmission $S_{21(s\text{-}as)}$ and $S_{21(s\text{-}mic)}$

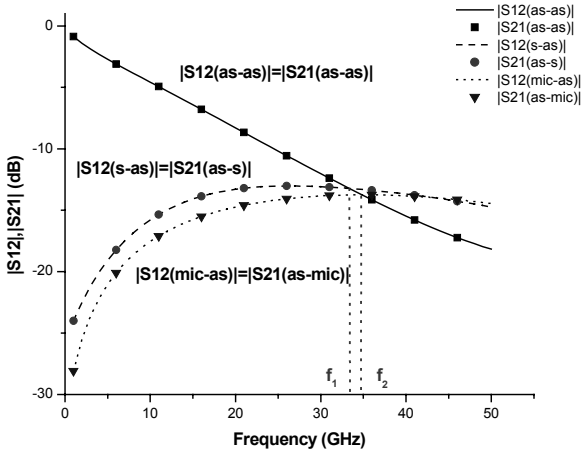

Fig.14 Magnitude of Mixed Mode transmission *s*-parameters of a metal layer transition on three coupled interconnects, antisymmetric–mode transmission $S_{21(as\text{-}as)}$ and the cross-modes transmission $S_{21(as\text{-}s)}$ and $S_{21(as\text{-}mic)}$

Comparison of these figures highlights the importance of mode conversion from 25 – 40 GHz in the case of symmetric and asymmetric mode propagation. Moreover, the conversion of microstrip mode is not as important as the others (in the microstrip mode conversion is reduced compared to the others). This results from the equivalent resistance value of each mode as shown by the difference in attenuation of the mode propagation *s*-parameters. Indeed, the equivalent resistance of the microstrip mode

is much weaker than the other one. Thus, the energy conversion of symmetric and antisymmetric modes in microstrip mode the energy conversion of microstrip mode is easier than the ennergy conversion of microstrip mode in the others. The microstrip mode fields configuration makes this phenomenon critical: indeed, in the case of a SOI technology, the return current would be partly carried out in the substrate.

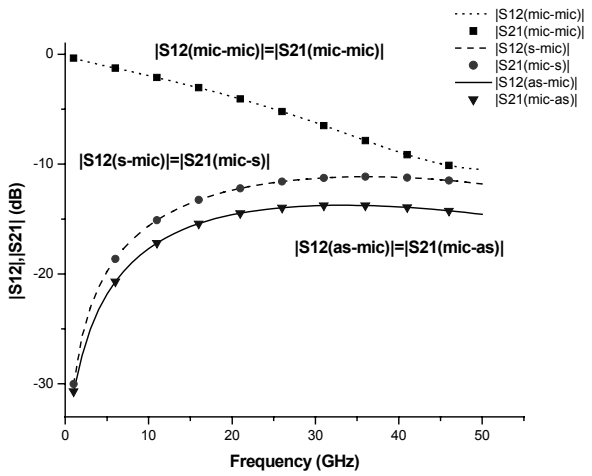

Fig.15 Magnitude of Mixed Mode transmission *s*-parameters of a metal layer transition bend on three coupled interconnects,
microstrip–mode transmission $S_{21(mic\text{-}mic)}$ and the cross-modes transmission $S_{21(mic\text{-}s)}$ and $S_{21(mic\text{-}as)}$

6. Conclusion

We investigated the communication, mode conversion at interconnects discontinuities in Digital ULSI circuits in order to determine simple rules for cross-mode reduction. The mode conversion analysis is indispensable to identify the signal return path, the return current distribution and therefore for an accurate inductance modeling The full wave analysis of two and three coupled interconnects showed that an important path difference implies an important cross-mode for a range frequency within about 25–40 GHz. Moreover, the time-domain circuit simulation illustrates the electromagnetic study. The mode conversion control has to reduce crosstalk and noise, and then, improves the IC Design quality.

7. References

[1] Y. I. Ismael , E. G Friedman, “Effect of inductance on propagation delay and repeater insertion in VLSI circuits” IEEE trans Very Large Scale Integration (VLSI) Systems, vol. 8 pp 195-206, April 2000.

[2] J. K. Wee, Y. J. Park, H. S. Min, D. H. Cho, M. H. Seung, “Modeling the Substrate Effect in Interconnect Line Characteristics of High Speed VLSI Circuits”, IEEE Trans. Microwave Theory and Tech., vol. MTT-46, no. 10, October 1998.

[3] I. Rahim, I. Lim, J. Foerstner, B. Y. Hwang, “Comparison of SOI versus bulk silicon substrate properties for mixed-mode IC’s”, in Proc. IEEE Int. SOI Conf, 1992, pp. 170-171.

[4] K. Joadar, “Comparison of SOI and junction isolation for substrate crosstalk suppression in mixed mode integrated circuits”, Electron. Lett., n° 15, pp. 1230-1231, July 1991.

[5] P. Pannier, L. Kadri, C. Seguinot, P. Kennis, F. Huret, “Accurate and efficient numerical method for the analysis of multimode waveguide discontinuities”, IEEE Trans. Microwave Theory and Tech., vol. MTT-48, no. 2, pp. 295-305, February 2000.

[6] Y. Quéré, T. Le Gouguec, P.M. Martin, D. Deschacht, F. Huret, “A simple design rule for substrate crosstalk reduction of high-speed VLSI Circuits”, Proceeding of the IEEE, signal propagation on interconnect, pp 151-154, Mai 2003.

[7] M. D. Wu, S. M. Deng, R. B. Wu, P. Hsu, “Full wave characterization of the mode conversion in a coplanar waveguide right-angled bend”, IEEE Trans. Microwave Theory and Tech., vol. MTT-43, pp. 2532-2538, November 1995.

[8] P. Pannier, E. Paleczny, P. Kennis, F. Huret, “Mode conversion at discontinuities in a microstrip coupled line waveguide”, Microwave and optical technology letters, Vol. 17, n°1, pp. 43-45, January 1998.

[9] E. Bockelman, W.R. Eisenstadt, “Combined Differential and Common-Mode Scattering Parameters: Theory and Simulation“, IEEE Transactions on Microwave Theory and Techniques, vol. 43, no.7, July 1995.

[10] J.F. Lee, D.K. Sun, Z.J. Cendes, “Full Wave Analysis of Dielectric Waveguies using Tangential Vector Finite Elements”, IEEE Trans. Microwave Theory and Tech., vol. MTT-39, no. 8, August 1991.